Journal of Urban and Environmental Engineering, v.11, n.2, p.142-149

ISSN 1982-3932
doi: 10.4090/juee. 2017.v11n2.142149

Journal of Urban and Environmental Engineering

www.journal-uee.org

THERMAL ANALYSIS OF URBAN ENVIRONMENTS IN MEDELLIN, COLOMBIA, USING AN UNMANNED AERIAL VEHICLE (UAV)

Engelberth Soto-Estrada*, Sebastián Correa-Echeveri and Martha Isabel Posada-Posada

[1]*Department of Civil Engineering, EIA University, Colombia*

Received 2 December 2016; received in revised form 2 February 2017; accepted 18 March 2017

Abstract: Thermal anomalies in built environments, known as Urban Heat Islands (UHI), are studied with satellite-derived data. However, this information is insufficient to examine regions such as the Aburra Valley, where the city of Medellin is located. In this valley, atmospheric interferences are common and the rugged terrain influences the amount of solar radiation reaching the surface, which hinders the analysis of the UHI. Unmanned Aerial Vehicles (UAVs) can be used to obtain the Land Surface Temperature (LST) at a time and location that is more convenient. In this project, a UAV was equipped with a thermal sensor to collect data on natural (ground vegetation and trees) and artificial (concrete, asphalt, and clay roof tiles) land cover types in Medellin, Colombia. The thermal information provided by the drone overcame the limitations of the satellite-derived data in terms of spatial, temporal, and radiometric resolution. This data enabled the study of specific land-cover types in different urban contexts, especially the influence of vegetation on LST. The findings suggested that the distribution of trees is crucial for UHI mitigation. Tree shading reduced the surface temperature of asphalt in average by 12°C and by 5.7°C for concrete. In addition, the presence of trees alongside streets reduced the maximum surface temperature of asphalt by 22.4°C in the same neighborhood. These results contributed to the understanding of the influence of urban development on Medellin's temperature.

Keywords: Heat Island Effect; UAV; Land Surface Temperature; Medellin

* Correspondence to: Engelberth Soto-Estrada, Tel.: +57 4 354 9090, Op. 1, Ext 878.
E-mail: engelberth.soto@eia.edu.co

INTRODUCTION

The Urban Heat Island (UHI) is a term used to describe the tendency of urban areas to experience higher outdoor air temperatures compared to the surrounding countryside (Landsberg, 1981). UHI is attributed to the urban landscape, including building density, size and orientation, open space configuration, and the use of heat-absorbing construction materials (Aleksandrowicz *et al.*, 2017; Asimakopoulos *et al.*, 2001; Erell *et al.*, 2011; Gartland, 2008).

UHI affects local ecosystems (Li *et al.*, 2016; Qaid *et al.*, 2016; Qunfang, 2015; Sarrat *et al.*, 2006), increases energy demand (Arifwidodo, 2015; Ihara *et al.*, 2008; Kolokothoni *et al.*, 2012), degrades air quality (USEPA, 2014), and increases the incidence of heat-related illnesses (Akbari, 2005; Bai *et al.*, 2014; Vieira-Araujo *et al.*, 2015). UHI can also exacerbate the impact of heat waves, which are periods of abnormally hot, and often humid, weather (USEPA, 2014).

Due to the above-mentioned facts, the mitigation of the UHI is a priority in cities such as New York (NYSERDA, 2006), Austin (ATG, 2016), Cambridge (City of Cambridge, 2015), Houston (Houston Advanced Research Center, 2009), and Toronto (EC2, 2008).

The environmental effects of the UHI may be higher in developing countries. Scott (2006) and Campbell-Lendrum and Corvalán (2007) indicated that the rapid economic development and the concurrent urbanization of poorer countries means that developing-country cities will be vulnerable to health hazards from both heat waves and UHI and simultaneously, an increasing contributor to the problem. The vulnerable city dwellers include those who live in houses built with lightweight (low thermal mass) construction materials and people with restricted access to air conditioning, refrigeration, and medical care.

UHI can be investigated through Land Surface Temperature (LST) values estimated from satellite-derived data (Tomlinson *et al.*, 2011). A wide range of sensors, e.g. Landsat 4, 5 (TM), 7 (ETM+), 8 (TIRS 1 and 2), Advanced Spaceborne Thermal Emission and Reflection (ASTER), Moderate Resolution Imaging Spectroradiometer (MODIS), Advanced Very High Resolution Radiometer (AVHRR), and others are used (Weng *et al.*, 2004). Nevertheless, atmospheric interferences and terrain morphology, which determine the solar radiation reaching the surface, and thus, the UHI intensity, affect LST estimations.

Medellin is located in a narrow valley (between 1120 and 3130 meters above mean sea level -AMSL) named after the river Aburra in the north-western part of Colombia. Soto-Estrada (2013) estimated Medellin's UHI using Landsat TM and ETM+ data. The results showed that the shape of the valley, especially the line of mountains running along either side of the valley in a north-south direction, influence the distribution of the UHI. The influence of the terrain was evident at the Landsat crossing time: 10:00 a.m. +/-15 minutes (USGS, 2016). At around 10:00 a.m. the valley's west side has received more solar radiation than the other side, which creates different LST patterns at local and regional scales.

Fig. 1 shows a 3D representation of the study region. The urban area was highlighted in dark gray. The image was shaded to represent light conditions at 10:00 a.m. This metropolitan region includes the city of Medellin (around 2.3 M inhabitants) and an agglomeration of neighboring urban municipalities such as Envigado in the south (about 185 000 citizens) and Bello in the north (approximately 400 000 inhabitants) (DANE, 2009).

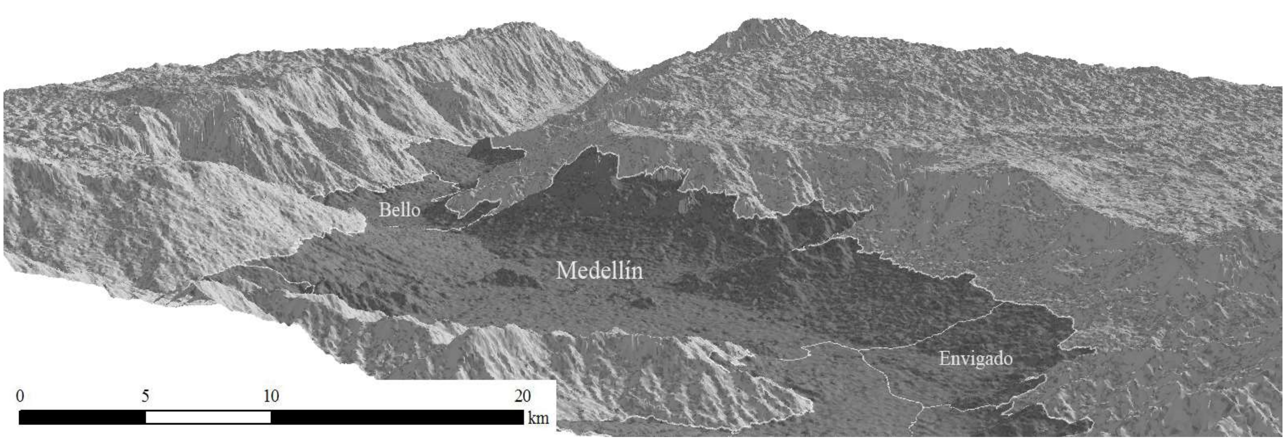

Fig. 1 3D view of the Aburra Valley and the urban area (in dark gray).

Unmanned Aerial Vehicles (UAVs), also known as drones, are small airborne platforms that can be equipped with several on-board sensors to get remotely sensed data at the desired time and spatial resolution. A drone equipped with a Fluke camera was used in this project to collect LST data of Medellin's common urban land cover types: concrete, asphalt, clay roof tiles, ground vegetation, and trees. The project´s main goal was to explore the advantages and disadvantages of using drones to investigate UHI in comparison with the satellite-derived information.

The next section of this article describes the methodology used to estimate the LST. Then, the results of the investigation are discussed, starting with a comparison between satellite and drone-derived LST data. The drone information is examined in detail, explaining the differences found between the LST data from different study areas. Finally, in the last section the main conclusions are outlined.

METHODOLOGY

The project was divided into four phases. In the first phase, all of the UAV's instrumentation and flight test activities were carried out. Flight missions were planned in the second step. The third phase was focused on the fieldwork, and the last one on data analysis.

A Tarot 650 Pro Hexacopter was equipped with a Fluke Ti100 thermal camera (7.5 to 14 µm spectral band). The metropolitan region was divided into a grid of 150 m square cells (see **0**), which were used to plan the flight missions. The grid-cell size was chosen to correspond to the drone's flight time.

Due to time and budget constraints, only five grid-cells were analyzed. A GIS-based multi-criteria decision analysis (MCDA) was used to select the study areas. The selection criteria included: terrain elevation, land use classification (residential, industrial, commercial, and services), accumulated solar radiation and safety-related aspects for UAV take-off and landing.

The flight path, speed, and altitude were determined according to the hexacopter's maximum flight time, (about 5 minutes with complete instrumentation), and the spatial resolution provided by the thermal sensor. At an altitude of 80 m, the Fluke camera acquired 40 meters (W) × 55.4 meters (H) imagery with a spatial resolution of 34 cm (see **0** and **0**).

Various methods were used to analyze the data collected. First, LST values derived from satellite (estimated in Soto-Estrada, 2013) and the UAV data were compared (see **0**). Then, 300 LST values were randomly extracted from each aerial image, as shown in **0**. These values, segmented by material, vegetation, and tree-shaded surfaces, were used to examine the influence of the surrounding built environment on LST. After that, a supervised classification method was performed to segment thermal information by land-cover as presented in **0**. A total of 25 images were processed obtaining more than 5000 LST values acquired on sunny days of September 2015 between 12:00 and 14:00 p.m.

RESULTS AND DISCUSSION

As shown in **0**, the LST data provided by the drone had better spatial (almost 100 times higher), temporal and radiometric resolution than Landsat 7. The Landsat sensor measures the amount of reflected energy for each 30 × 30 m area (NASA, 2006), which, at the scale of area presented in **0**, only produced two LST values (30.5 and 30.7°C). In contrast, the Fluke sensor provided a detailed thermal image (34 cm spatial resolution), which revealed a range of surface temperatures from 26.5 to 74.9°C.

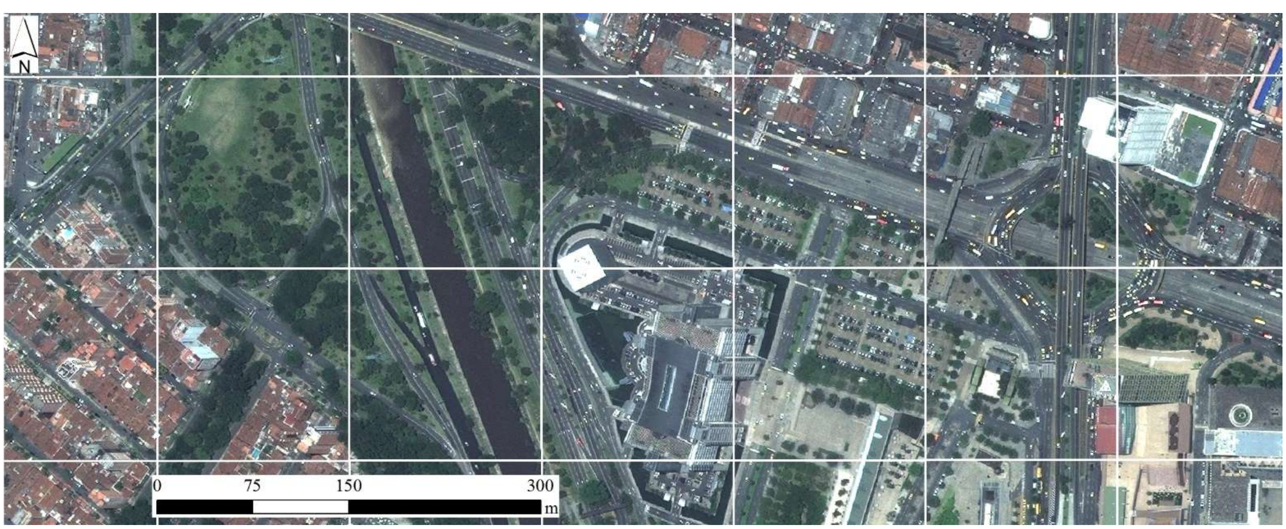

Fig. 2 Grid of 150 m square cells over Medellin for the selection of study areas.

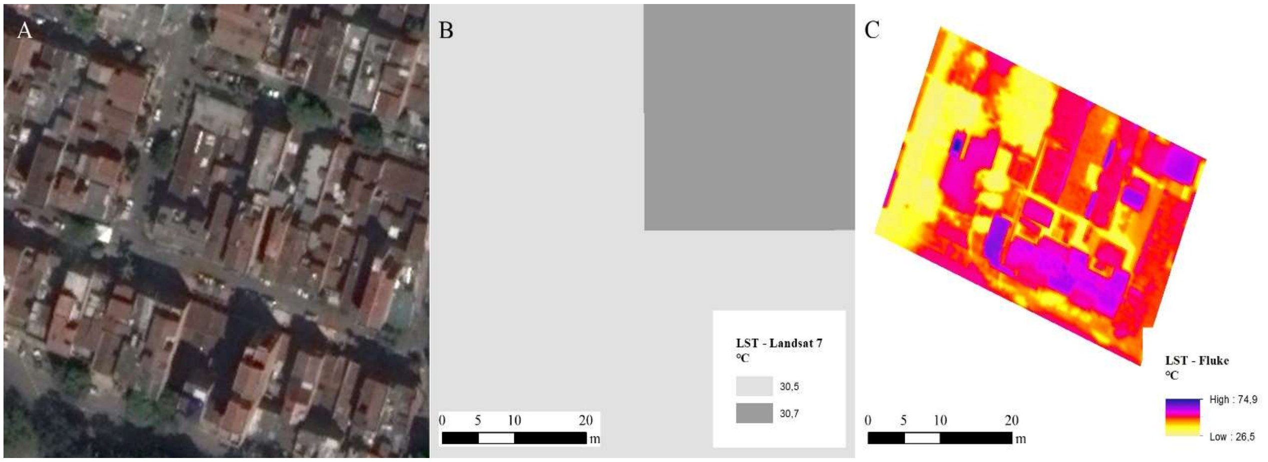

Fig. 3 Comparison between LST values derived from Landsat 7 (B) and the thermal sensor used in this study (C).

Fig. 4 Thermal image (34 cm spatial resolution) of a residential locality of Medellin and random sampling points.

0 compiles average LST values by land-cover type and study area (grid-cell). **0** summarizes physical conditions and other characteristics of the study areas.

As shown in **0**, all flights were carried out under similar conditions of air temperature and solar intensity. That was a prerequisite for this study and the reason to use a drone to get LST data. The use of an MCDA ensured that the selected grid-cells represent the urban landscape of Medellin, especially vegetation cover, building typology, and terrain elevation (see **0**).

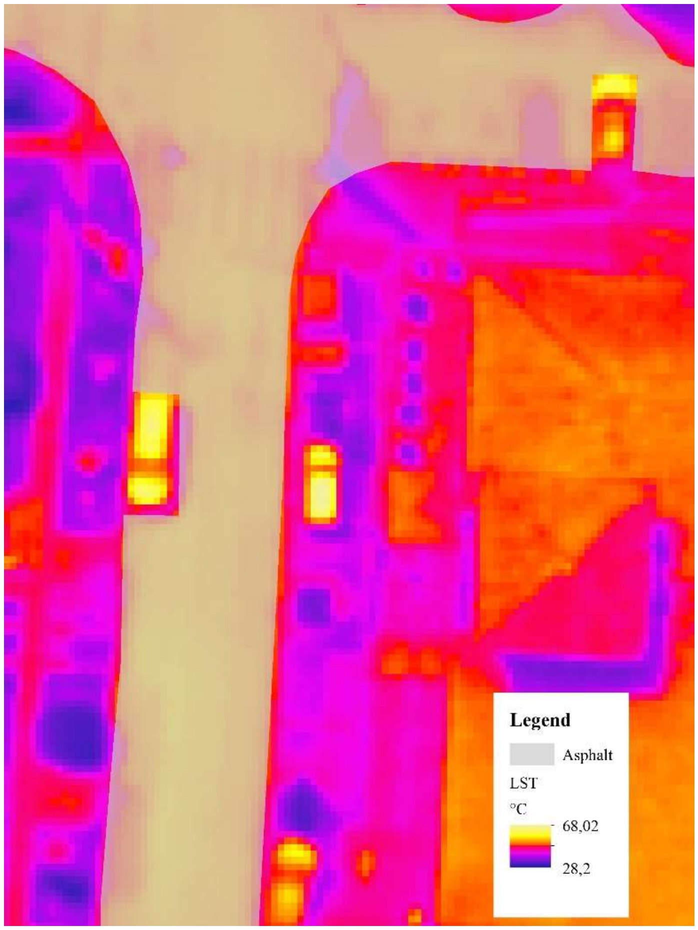

Fig. 5 Thermal image of the same locality shown in 0 and segmented area for asphalt analysis.

Table 1. Average LST values by land-cover and study area (grid-cell)

Land cover	Average LST by study area (°C)					Number of sampling points	Average temperature (°C)
	1	2	3	4	5		
Asphalt	51.35	38.66	51.76	52.88	51.40	979	49.21
Concrete	43.24	38.82	47.33	47.94	45.19	762	44.51
Clay roof tiles	46.81	41.43	49.05	-	47.12	1535	46.10
Ground vegetation	36.03	34.61	34.68	32.27	31.19	860	33.76
Tree canopy	32.49	28.68	33.49	32.46	31.28	300	31.68

Table 2. Physical conditions and other characteristics of the study areas during flight missions

Study area	Predominant land-use	Elevation average (AMSL)	Solar radiation (Wh/m^2)	Humidity (%)	Wind speed (m/s)	Air temperature (°C)	Vegetation cover (%)
1	Residential	1477	795	43.7	2.4	29.9	32.4
2	Residential	1481	824	41.2	2.4	30.7	36.7
3	Residential	1467	796	54.0	0	31.8	13.8
4	Industrial	1455	804	33.4	0.6	31.9	17.3
5	Residential	1706	849	38.8	4.4	31.0	20.3

Fig. 6 Study areas (150 m square).

Four study areas were chosen in the lowest part of the valley where most of the urban population is located, and one grid-cell on the east-facing hillside (see **Fig. 1**).

The vegetation cover was estimated from a WorldView-2 satellite image (4 bands: red, green, blue, and near-infrared; 50 cm spatial resolution). According to that estimation, the study areas 1 and 2 had approximately one-third of their surface covered by vegetation (see **0**), which is common in the upper-income neighborhoods of Medellin. The grid-cell 3 belongs to the typical middle-income communities (14% vegetation cover), the study area 4 to the traditional industrial district located alongside the Aburra River (17% vegetation cover), and the study area 5 to the average upper-income neighborhoods located on the south-east hillsides of the city of Medellin (20% vegetation cover). **0** displays the study areas.

As indicated in **0**, the average LST was similar in four out to five study areas even though their land-cover composition was different (see **0**). For instance, study areas 1 and 3 had similar LST average values but different extent of vegetation cover (32.4 and 13.8%, respectively).

Surface temperatures were lower in the study area 2 compared with the other study locations, especially for concrete and asphalt surfaces. The study areas 1 and 2 can be directly compared since they belong to the same locality (see **0**), and because the thermal information was acquired under similar conditions as reported in **0**.

The average surface temperature (AST) of asphalt in the study area 2 was 12.7°C lower than the average value in the study area 1. A difference of 4.4°C was estimated between the AST of concrete in these two study areas.

Comparing the statistical mode (see **0**), in the study area 2 asphalt temperature was 12.8°C lower than in study area 1, while the minimum and maximum temperatures had a difference of 6.1 and 22.4°C between the two study areas, respectively.

These outcomes can be related to the composition of the vegetation cover (ground vegetation - trees) and are

Table 3. Asphalt surface temperature statistics

Study area	Number of pixels analyzed	Asphalt temperature [°C]		
		Minimum	Maximum	Mode
1	1645	38.3	65.0	53.8
2	1403	32.2	42.6	41.0
3	2143	31.5	64.3	52.5
4	833	32.4	57.3	56.0
5	2076	28.8	55.1	52.6

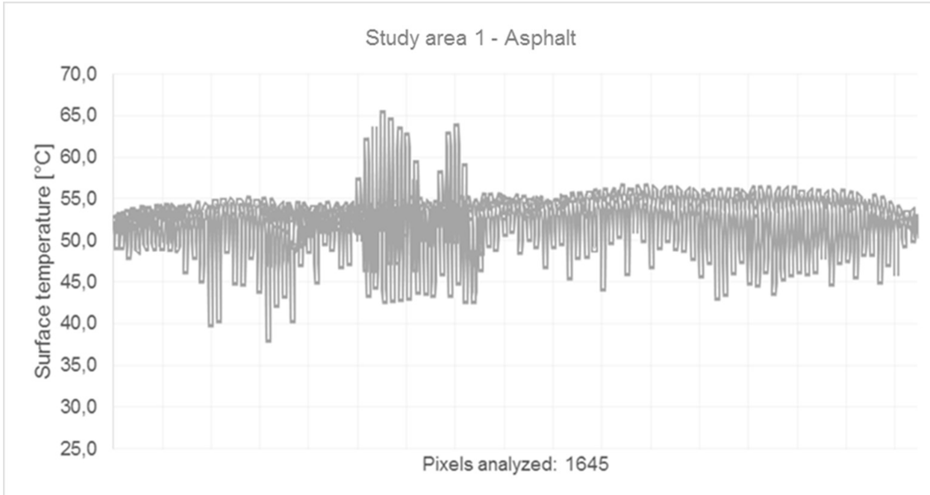

Fig. 7 Distribution of surface temperature of asphalt in study area 1.

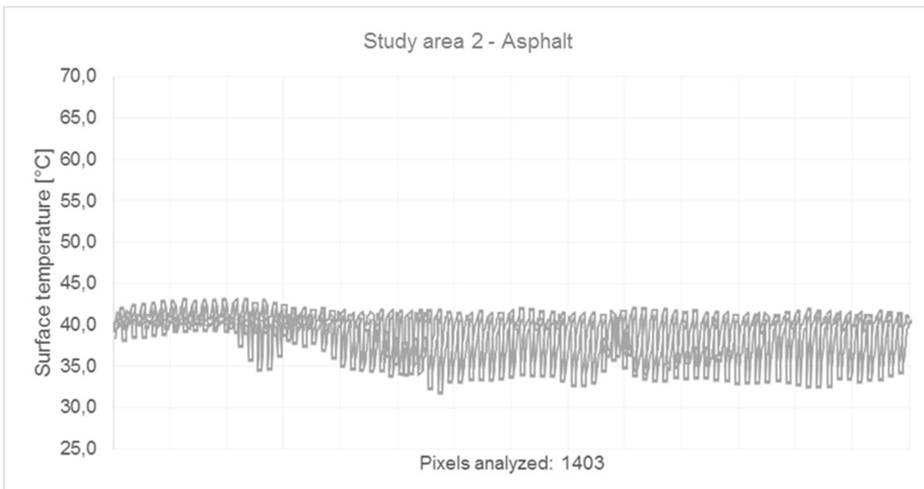

Fig. 8 Distribution of surface temperature of asphalt in study area 2.

in line with the findings of Berry *et al.*, (2013), Shashua-Bar *et al.* (2009), Sawka *et al.*, (2013), and Kieron & Hutchings (2013). These authors studied the importance of vegetation (particularly trees) in temperature abatement and energy conservation.

The use of vegetation as UHI mitigation strategy is very well known (USEPA, 2014). Shade trees reduce the heat absorbed by urban surfaces. In addition, trees release vapor to the atmosphere through evapotranspiration, increasing the relative humidity and reducing the air temperature around them; this, in turn, can lead to a local increase in thermal comfort (Aleksandrowicz *et al.*, 2017).

In both study areas (1 and 2) housing, streets, and green areas are the predominant land cover types (see **0**). However, the spatial distribution of vegetation in study area 2 is delimited by the street layout. This distribution helped to reduce the surface temperature of concrete and asphalt. While the maximum surface temperature of asphalt was 65°C in the study area 1, it was 22.4°C higher in comparison to study area 2.

0–8 show the distribution of asphalt temperatures in the study areas 1 and 2. In addition to the distribution of vegetation, the results suggested that the vegetation composition (ground vegetation - trees) was also a factor in the reduction of surface temperature.

Tree canopy covered 22% of the study area 2, seven percent more than the extent of canopy cover in the study area 1. **0** clearly illustrates the effect of tree shading on LST. Considering the data obtained in the five study areas, it was estimated that tree shading reduced the surface temperature of asphalt by 12°C and by 5.7°C for concrete.

CONCLUSIONS

The use of a drone equipped with a thermal camera was a good alternative to overcome the limitations of the satellite-derived data in terms of spatial, temporal and radiometric resolution. The Fluke sensor provided detailed thermal information (34 cm spatial resolution) on the urban landscape of Medellin.

This approach enabled the study of specific land cover types in different urban contexts. The analysis of the influence of vegetation on LST showed that the distribution of trees is crucial for UHI mitigation. Tree shading reduced the surface temperature of asphalt in average by 12°C and by 5.7°C for concrete. In addition, the presence of trees alongside streets reduced the maximum surface temperature of asphalt by 22.4°C in the same neighborhood.

These findings contribute to the understanding of the urban forest environmental services in Medellin, which go beyond the production of oxygen or the conservation of flora and fauna, they also include air temperature regulation in built-up urban environments.

However, to determine the influence of LST on air temperature a large amount of information is required, which becomes a major limitation to the drone technology.

Considering the new UAV's safety regulations in Colombia, for flights in urban areas, and the technical challenges faced during this project to obtain spare parts, the use of a bigger aerial platform, like a helicopter or a light plane, to get enough thermal information from broad areas of the Aburra Valley is highly recommended.

Acknowledgment. The authors would like to thank the EIA University for funding this project.

REFERENCES

Akbari, H. (2005). Energy saving potentials and air quality benefits of urban heat island mitigation. *Lawrence Berkeley National Laboratory*, 19.

Aleksandrowicz, O., Vuckovic, M., Kiesel, K., & Mahdavi, A. (2017). Current trends in urban heat island mitigation research: Observations based on a comprehensive research repository. *Urban Climate, 20*.

Arifwidodo, S., (2015). Urban heat island and household energy consumption in Bangkok, Thailand. *Energy Procedia*, **79**, 189–194.

Asimakopoulos, D., Assimakopoulos, V., Chrisomallidou, N., Klitsikas, N., Mangold, D., Michel, P., & Tsangrassoulis, A. (2001). *Energy and Climate in the Urban Built Environment.* London: James & James.

ATG. (2016). *The Heat Island Effect: Cooling strategies*. Retrieved from https://www.austintexas.gov/coolspaces

Bai, L., Ding, G., Gu, S., Bi, P., Su, B., Qin, D., & Liu, Q. (2014). The effects of summer temperature and heat waves on heat-related illness in a coastal city of China, 2011–2013. *Environmental Research*, **132**, 212–219.

Berry, R., Livesley, S. J., & Aye, L. (2013). Tree canopy shade impacts on solar irradiance received by buildings walls and their surface temperature. *Building and Environment*, **69**, 91–100.

Campbell-Lendrum, D., & Corvalán, C. (2007). Climate change and developing-country cities: Implications for environmental health and equity. *Journal of Urban Health: Bulletin of the New York Academy of Medicine*, **84**(1), 109–115.

City of Cambridge. (2015). *Climate Protection Action Committee.* Cambridge: City of Cambridge.

DANE. (2009). *Colombia. Proyecciones de población municipales por área.* Bogotá: DANE.

EC2. (2008). *Urban Heat Island Mitigation Strategy Toolkit.* Toronto: Ryerson School of Urban and Regional Planning.

Erell, E., Pearlmutter, D., & Williamson, T. (2011). *Urban Microclimate: Designing the spaces between buildings.* Washington, DC: Earthscan.

Gartland, L. (2008). *Heat islands: Understanding and mitigating heat in urban areas.* London: Earthscan.

Houston Advanced Research Center. (2009). *Dallas urban heat island.* The Woodlands: Houston Advanced Research Center.

Ihara, T., Kikegawa, Y., Asahi, K., & Genchi, Y. (2008). Changes in year-round air temperature and annual energy consumption in office building areas by urban heat-island countermeasures and energy-saving measures. *Applied Energy*, **85**(1), 12–25.

Kieron, D., & Hutchings, T. (2013). *Air temperature regulation by urban trees and green infrastructure.* Surrey: UK Forestry Commission.

Kolokothoni, M., Ren, X., & Davies, M. (2012). London's urban heat island: Impact on current and future energy consumption in office buildings. *Energy Buildings*, **47**, 302–311.

Landsberg, H. E. (1981). *The Urban Climate.* New York: Academic Press.

Li, X., Li, W., Middel, A., Harland, S. L., & Brazel, A. J. (2016). Remote sensing of the surface urban heat island and land architecture in Phoenix Arizona: Combined effects of land composition and configuration and cadastral-demographic-economic factors. *Remote sensing of environment*, **174**, 233–243.

NASA. (2006). *How Landsat images are made.* Washington, DC: NASA.

NYSERDA. (2007). *New York City Regional Heat Island Initiative*. Retrieved from https://www.nyserda.ny.gov/-/media/Files/Publications/Research/Environmental/EMEP/NYC-Heat-Island-Mitigation.pdf.

Qaid, A., Bin-Lamit, H., Remaz-Ossen, D., Nafida, R., & Shahminan, R. (2016). Urban heat island and thermal comfort conditions at micro-climate scale in a tropical planned city. *Energy and Buildings*, 133, 577–295.

Qunfang, H. (2015). The effect of urban heat island on climate warming in the Yangtze River Delta Urban Agglomeration in China. *International Journal of Environment Research and Public Health*, **12**(8), 8773–8789.

Sarrat, C., Lemonsu, A., Masson, V., & Guedalia, D. (2006). Impact of urban heat island on regional atmospheric pollution. *Atmospheric Environment*, **40**(10), 1743–1758.

Sawka, M., Millward, A. A., McKay, J., & Sarkovich, M. (2013). Growing summer energy conservation through residential tree planting. *Landscape and Urban Planning*, 113, 1–9.

Scott, M. (2006). *Earth observatory*. Retrieved from http://earthobservatory.nasa.gov/Features/GreenRoof/

Shashua-Bar, L., Pearlmutter, D., & Errel, E. (2009). The cooling efficiency of urban landscape strategies in a hot dry climate. *Landscape Urban Plan*, **92**(3-4), 179–186.

Soto-Estrada, E. (2013). Regresión ponderada geográficamente para el estudio de la temperatura superficial en Medellín, Colombia. *Revista AIDIS*, **6**(3), 42–53.

Tomlinson, C. J., Chapman, L., Thornes, J. E., & Baker, C. (2011). Remote sensing land surface temperature for meteorology and climatology: A review. *Metereological Applications*, **18**(3), 296–306.

USEPA. (2014). *Reducing urban heat islands: Compendium of strategies.* Retrieved from https://www.epa.gov/heat-islands/heat-island-compendium.

USGS. (2016, 29 November). *Landsat 8*. Retrieved from https://landsat.usgs.gov/landsat-8-history

Vieira-Araujo, R., Albertini, M., Costa-da-Silva, A., Suesdek, L., Soares-Franceschi, N., & Marcal, N. (2015). Sao Paulo urban heat islands have a higher incidence of dengue than other urban areas. *The Brazilian Journal of Infectious Diseases*, **19**(2), 146–155.

Weng, Q., Lu, D., & Schubring, J. (2004). Estimation of land surface temperature – vegetation abundance relationship for urban heat island studies. *Remote Sensing of Environment* **89**(4), 467–483.